

Novel TRKB agonists activate TRKB and downstream ERK and AKT signaling to protect A β -GFP SH-SY5Y cells against A β toxicity

Ya-Jen Chiu^{1,*}, Te-Hsien Lin^{1,*}, Kuo-Hsuan Chang², Wenwei Lin³, Hsiu Mei Hsieh-Li¹, Ming-Tsan Su¹, Chiung-Mei Chen², Ying-Chieh Sun³, Guey-Jen Lee-Chen¹

¹Department of Life Science, National Taiwan Normal University, Taipei 11677, Taiwan

²Department of Neurology, Chang Gung Memorial Hospital, Chang Gung University College of Medicine, Taoyuan 33302, Taiwan

³Department of Chemistry, National Taiwan Normal University, Taipei 11677, Taiwan

*Equal contribution

Correspondence to: Chiung-Mei Chen, Ying-Chieh Sun, Guey-Jen Lee-Chen; email: cmchen@cgmh.org.tw, sun@ntnu.edu.tw, t43019@ntnu.edu.tw

Keywords: Alzheimer's disease, TRKB agonists, A β , neuroprotection, therapeutics

Received: February 18, 2022

Accepted: September 17, 2022

Published: September 26, 2022

Copyright: © 2022 Chiu et al. This is an open access article distributed under the terms of the [Creative Commons Attribution License](https://creativecommons.org/licenses/by/3.0/) (CC BY 3.0), which permits unrestricted use, distribution, and reproduction in any medium, provided the original author and source are credited.

ABSTRACT

Decreased BDNF and impaired TRKB signaling contribute to neurodegeneration in Alzheimer's disease (AD). We have shown previously that coumarin derivative LM-031 enhanced CREB/BDNF/BCL2 pathway. In this study we explored if LM-031 analogs LMDS-1 to -4 may act as TRKB agonists to protect SH-SY5Y cells against A β toxicity. By docking computation for binding with TRKB using 7,8-DHF as a control, all four LMDS compounds displayed potential of binding to domain d5 of TRKB. In addition, all four LMDS compounds exhibited anti-aggregation and neuroprotective efficacy on SH-SY5Y cells with induced A β -GFP expression. Knock-down of TRKB significantly attenuated TRKB downstream signaling and the neurite outgrowth-promoting effects of these LMDS compounds. Among them, LMDS-1 and -2 were further examined for TRKB signaling. Treatment of ERK inhibitor U0126 or PI3K inhibitor wortmannin decreased p-CREB, BDNF and BCL2 in A β -GFP cells, implicating the neuroprotective effects are via activating TRKB downstream ERK, PI3K-AKT and CREB signaling. LMDS-1 and -2 are blood-brain barrier permeable as shown by parallel artificial membrane permeability assay. Our results demonstrate how LMDS-1 and -2 are likely to work as TRKB agonists to exert neuroprotection in A β cells, which may shed light on the potential application in therapeutics of AD.

INTRODUCTION

Alzheimer's disease (AD) is the most common disorder that causes dementia. Amyloid β (A β)-containing plaques and neurofibrillary tangles deposited in the brains are the main pathological features [1]. Several mutations in the A β precursor protein (APP) and presenilin-1 (PS1) and -2 (PS2) genes have been shown to cause familial AD [2]. A β deposition is one of the early events in AD pathology [3]. APP is an integral membrane protein that is proteolyzed to generate a peptide containing 39–43 amino acids. The A β peptide

composed of 42 amino acids (A β 42) is the main peptide accumulated in the AD brains [4]. A β monomer misfolds into oligomers, pre-fibrillar and insoluble fibrillar aggregates that are toxic to neurons [5, 6]. The accumulated misfolded proteins cause neurotoxicity that leads to apoptosis [7, 8]. Thus, clearance of the abnormal A β aggregates has been suggested as a therapeutic method to modify disease progression in AD.

Brain-derived neurotrophic factor (BDNF), a neurotrophic factor, is expressed ubiquitously in whole

brain and plays a vital role in promoting neural plasticity, neuronal growth and cell survival [9]. BDNF has a high binding affinity to tropomyosin-related kinase B (TRKB), also known as neurotrophic receptor tyrosine kinase 2, to induce TRKB dimerization and phosphorylation of TRKB, and subsequently to activate downstream cascades including, phosphoinositide 3-kinase (PI3K)-AKT serine/threonine kinase (AKT), extracellular signal-regulated kinase (ERK)-cAMP responsive element binding protein 1 (CREB), and phospholipase C- γ 1 (PLC- γ 1). The TRKB receptor activation would lead to enhanced memory formation and storage as well as neuroplasticity, neurogenesis, neurite outgrowth and neuronal survival [10, 11]. ERK phosphorylates CREB to promote transcription of genes for neuronal survival, neurite outgrowth and neuroplasticity [12], such as BDNF [13] and BCL2 apoptosis regulator (BCL2) [14]. The post-synaptic ERK signal would also enhance the neuroplasticity related long-term potentiation [11].

Decreased BDNF has been shown in several neurodegenerative diseases [12]. Previous reports have shown that BDNF transcription and protein expression is reduced in hippocampus, cortex and Meynert basal ganglion of AD brains [13, 14]. It has been shown that accumulation of A β is associated with loss of BDNF [15] and A β inhibits protein kinase A to down-regulate the CREB phosphorylation and expression of BDNF [15, 16]. Oligomeric A β also interferes with Ras-ERK and PI3K-AKT pathways to aggravate neurotoxicity [17]. Several preclinical studies using AD mouse models have demonstrated that increased BDNF expression rescues neurotoxicity and improves cognitive function [18–20]. Nevertheless, the poor bioavailability of BDNF, or example the short half-life in plasma and the limited blood–brain barrier (BBB) permeability [21], restricts the application of BDNF.

Developing novel small molecule agonists of TRKB receptor is a potential therapeutic strategy for neurodegenerative diseases including AD [22]. To identify compounds acting as TRKB agonists with a good BBB permeability is crucial for developing therapeutics for AD. Our previous studies have demonstrated that a novel coumarin derivative, LM-031, displayed neuroprotective effects by upregulating CREB/BDNF/BCL2 pathway in our Flp-In A β -GFP SH-SY5Y cells [23]. In this study, we searched three online databases for LM-031 analogous compounds using compound similarity search software tools and identified four top-scoring compounds LMDS-1 to -4 as the candidate TRKB agonists. To examine their plausible role as TRKB agonists, docking computation was firstly conducted to investigate binding strength

and conformation of LM-031 and the four analogs. We then examined if the four potential small TRKB agonists would exert neuroprotective effects and influence the TRKB downstream pathways in A β -GFP folding reporter SH-SY5Y cells. The BBB permeability was also examined by using parallel artificial membrane permeability assay (PAMPA).

RESULTS

Test compounds

We tested the coumarin derivative LM-031 and the analogs LMDS-1 to -4 (Figure 1A). According to their molecular weight (MW), hydrogen bond acceptor (HBA), hydrogen bond donor (HBD), and octanol-water partition coefficient (cLogP), these five compounds fulfill five criteria of Lipinski's rule for predicting oral bioavailability [24] (Figure 1B). All five compounds were anticipated to diffuse over the BBB with a polar surface area (PSA) of smaller than 90 Å² [25], which were similarly supported by an online BBB predictor [26] (Figure 1B).

Anti-amyloid and anti-oxidative stress are regarded as crucial AD therapeutic approaches. The thioflavin T fluorescence assay was applied to gauge the suppression of A β aggregation. Curcumin is known to reduce amyloid aggregation [27]. Both curcumin and coumarin were included for comparison. Half maximal effective concentration (EC₅₀) values of curcumin, LM-031, LMDS-1 to -4 and coumarin to inhibit A β aggregation were: <5, 9, <5, 18, 14, <5 and 25 μ M, respectively (Figure 1C). The free radical scavenging activity of the LM-031, analogs and coumarin was investigated using diphenylpicrylhydrazyl (DPPH) as a substrate. Kaempferol (a positive control [28]), LM-031, LMDS-1 to -4 and coumarin had EC₅₀ values of 28, 104, 117, 146, 167, 116 and 179 μ M, respectively (Figure 1D).

Binding strength and conformation by docking computation

Figure 2A shows the binding conformations of 7,8-DHF, LM-031 and two representative LMDS compounds (LMDS-1 and -4) and Figure 2B shows the predicted binding strengths of these compounds. Of the tested compounds, the computations predicted that LMDS-1 and -2 were the top two compounds interacting with TRKB receptor. Note that the LMDS compounds have different binding modes in comparison with 7,8-DHF and LM-031. In addition, interestingly, all LMDS-1 to -3 have the same binding mode, 3 hydrogen bonds with backbone of L315 and I334, and side chain of K312. In contrast, LMDS-4 binds with d5

domain in different orientation with a lower binding strength compared with LMDS-1 to -3. It only has a bifurcated hydrogen bond with side chain of K312. These results suggest that bulky carboxylate group is not favorable functional group at the position of fused ring of LMDS compounds shown in Figure 1A.

A β aggregation inhibition and reduction of A β -induced oxidative stress

A β -GFP SH-SY5Y cells [29] were used to examine A β aggregation inhibition of LM-031 and analogs (Figure 3A). The cell model uses GFP as a reporter to

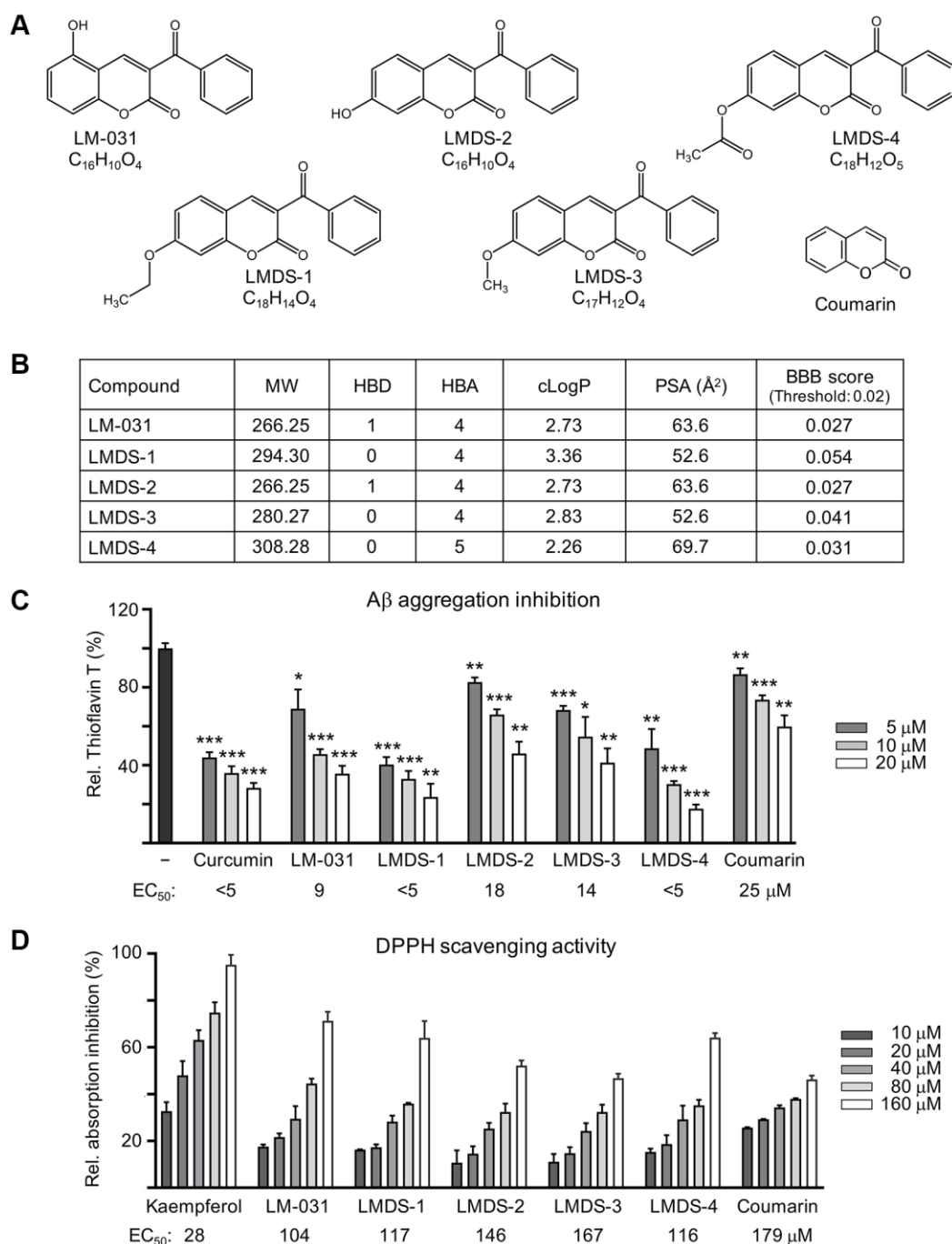


Figure 1. LM-031 and analogous compounds. (A) Structure and formula of LM-031 and analogs LMDS-1 to -4 and coumarin backbone. (B) Molecular weight (MW), hydrogen bond donor (HBD), hydrogen bond acceptor (HBA), calculated octanol-water partition coefficient (cLogP), polar surface area (PSA), and predicted blood-brain barrier (BBB) score of these compounds. (C) A β aggregation inhibition of curcumin (as a positive control), coumarin, LM-031 and analogs (5–20 μ M) by the thioflavin T assay ($n = 3$). To normalize, the relative thioflavin T fluorescence of A β ₄₂ without compound treatment was set at 100%. Shown below are the EC₅₀ values. (D) Radical scavenging activity of kaempferol (as a positive control), coumarin, LM-031 and analogs (10–160 μ M) on DPPH ($n = 3$). Shown below are the EC₅₀ values.

reflect the level of A β misfolding. The fast misfolding and formation of A β aggregates causes misfolding of fused GFP, thereby suppressing green fluorescence. Compounds that inhibit A β misfolding allow refolding of GFP monitored by an increase in green fluorescence on A β -GFP expressing cells [30]. Curcumin, which can modify the A β aggregation pathway and ameliorate A β -induced toxicity [31], was considered as a positive control. Coumarin was also included for comparison.

The intensity of GFP fluorescence in cells pre-treated with 2.5–5 μ M curcumin and 1.2–5 μ M coumarin was significantly increased (113–140%, $P = 0.037$ –0.001; cell viability: 101–91%) compared to the untreated cells (100%). Treatment with LM-031, LMDS-1, -2, -4 at 1.2–5 μ M, or LMDS-3 at 2.5–5 μ M significantly increased the intensity of green fluorescence (111–149%, $P = 0.048$ –0.001; cell viability: 106–92%) (Figure 3B), while A β -GFP RNA level was not affected

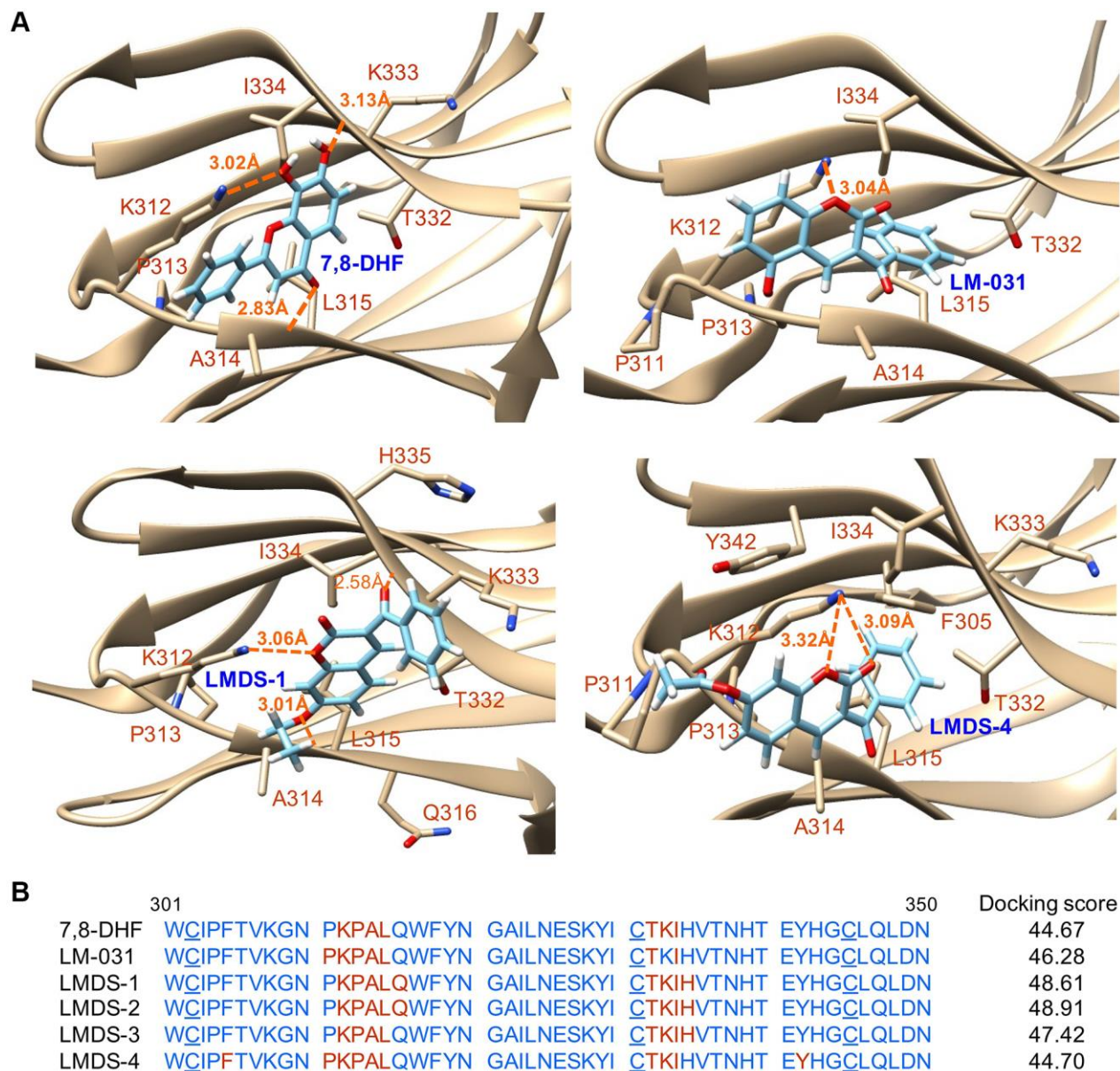


Figure 2. Docking computations of 7,8-DHF, LM-031 and analogs. (A) The docking conformations of 7,8-DHF (as a positive control), LM-031, LMDS-1 and LMDS-4 binding to extracellular d5 domain (the second immunoglobulin-like domain, residues 250–340) of TRKB receptor. The TRKB-d5 domain (ribbon structures) is colored in beige and the wire-frame structures denote the compounds. The labeled amino acids were within 10 Å radii of examined compounds. Carbon, oxygen, hydrogen and nitrogen atoms of compounds or side chains of surrounding amino acids are shown in light blue, red, white and blue, respectively. The dotted orange lines indicate hydrogen bond interactions between compounds and protein. (B) Amino acid residues 301–350 of d5 domain. The amino acids within 10 Å radii of examined compounds are colored in red; the cysteines involved in disulfide linkage are underlined. Shown on the right were docking scores of 7,8-DHF, LM-031 and analogs calculated by the GOLD program.

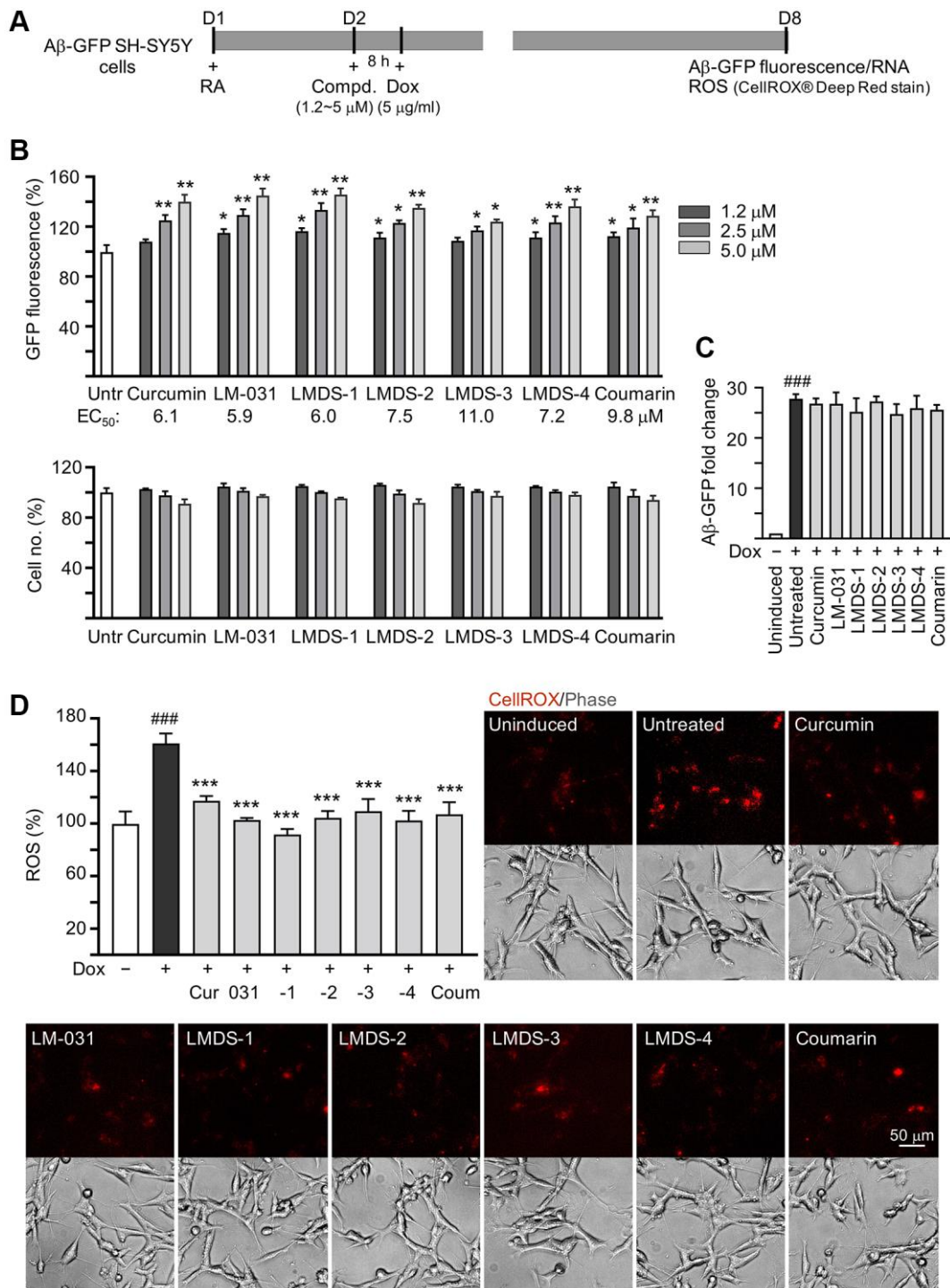


Figure 3. Aβ aggregation and oxidative stress inhibitory effects of LM-031 and analogs in Aβ-GFP SH-SY5Y cells. (A) Experimental flow chart. On day 1, cells were plated with retinoic acid (RA, 10 μM) added to the culture medium. On day 2, curcumin, coumarin, LM-031 or analogs (1.2–5 μM) was added to the cells for 8 h, followed by inducing Aβ-GFP expression with doxycycline (Dox, 5 μg/ml) for 6 days. On day 8, Aβ-GFP fluorescence, Aβ-GFP RNA and ROS (CellROX® Deep Red stain) were measured. (B) Assessment of GFP fluorescence with curcumin, coumarin, LM-031 or analogs (1.2–5 μM) treatment ($n = 3$), with EC₅₀ values shown below. Shown underneath are cell number analyzed in each treatment. The relative GFP fluorescence/cell number of untreated cells (Untr) was normalized as 100%. (two-tailed Student's t test; * $P < 0.05$ and ** $P < 0.01$) (C) Aβ-GFP RNA of Aβ-GFP SH-SY5Y cells untreated or treated with curcumin, coumarin, LM-031 or analogs at 5 μM ($n = 3$). HPRT1 was used for normalization. (D) Images of CellROX® Deep Red stain (red) and ROS assay of Aβ-GFP cells uninduced, untreated, or treated with curcumin, coumarin, LM-031 or analogs at 5 μM ($n = 3$). The relative ROS of uninduced cells (Dox-) was normalized (100%). (C, D) P values: comparisons between induced (Dox+) vs. uninduced (Dox-) cells (### $P < 0.001$), or compound-treated vs. untreated (Dox+) cells (** $P < 0.001$). (one-way ANOVA with *post hoc* Tukey test).

by LM-031 and analogs at 5 μ M concentration (24.8–27.3 folds, $P > 0.05$) (Figure 3C). For A β aggregation inhibition, curcumin, LM-031, LMDS-1 to -4 and coumarin had EC₅₀ values of 6.1, 5.9, 6.0, 7.5, 11.0, 7.2 and 9.8 μ M, respectively. In an analysis of oxidative stress, the level of reactive oxygen species (ROS) increased significantly in A β -GFP-expressing SH-SY5Y cells (161%, $P < 0.001$), while treatments with curcumin, LM-031, analogs and coumarin at a concentration of 5 μ M decreased the ROS level induced by induced A β expression (117–92%, $P < 0.001$) (Figure 3D). These results indicated that the LM-031 and analogs not only hindered the aggregation of amyloid, but also attenuated oxidative stress caused by A β overexpression.

Neuroprotective activity of LM-031 and analogs

The neuroprotective efficacy of LM-031 and analogs, including acetylcholinesterase (AChE) and caspase 1 activity, and neurite outgrowth, were evaluated. A β overexpression significantly reduced length (from 30.6 μ m to 23.1 μ m, $P = 0.002$), process (from 3.9 to 3.0, $P = 0.005$) and branch (from 3.0 to 2.0, $P = 0.002$) of neurites. Respective curcumin, LM-031 or analogs (5 μ M) treatment successfully increased neurite length (from 23.1 μ m to 27.5–31.2 μ m, $P = 0.036$ – <0.001) and branch (from 2.0 to 2.7–2.9, $P = 0.047$ – 0.006), while rescue of process was evident only for curcumin and LM-031 (from 3.0 to 3.7–3.8, $P = 0.011$ – 0.002) (Figure 4A). AChE (120%, $P = 0.007$) and caspase 1 (153%, $P < 0.001$) activities were also considerably elevated by A β overexpression, whereas treatment with curcumin, LM-031 and analogs (5 μ M) decreased AChE (from 120% to 103–83%; $P = 0.027$ – <0.001) and caspase 1 (from 153% to 137–115%; $P = 0.014$ – <0.001) activities in comparison to no treatment (Figure 4B).

TRKB knockdown in A β -GFP-expressing SH-SY5Y cells

Next, we used lentivirus-mediated shRNA targeting to knock down TRKB expression to assess the role of TRKB and downstream signaling (Figure 5A), since the investigated TRKB agonists had neuroprotective activity on A β -GFP-expressing SH-SY5Y cells. A β -GFP overexpression had no significant impact on TRKB expression in cells infected with control (scrambled) shRNA (72%; $P > 0.05$). TRKB expression was unaffected by treatment with LM-031 and analogs (97–106%; $P > 0.05$). In contrast, TRKB-specific shRNA decreased the amount of TRKB in A β -GFP-expressing cells without (from 75% to 30%, $P = 0.002$) or with (from 97–106% to 28–32%; $P < 0.001$) LM-031 and analogs treatment (Figure 5B).

In addition to examining the level of TRKB, the levels of downstream signaling effectors including ERK, AKT and CREB in TRKB-knockdown cells in response to treatment with LMDS compounds were also examined (Figure 5C). A β -GFP overexpression decreased the expression of p-ERK (47%, $P < 0.001$), p-AKT (46%, $P < 0.001$), and p-CREB (48%, $P = 0.002$) in cells infected with scrambled shRNA, and the reduction was not worsened by TRKB-specific shRNA infection ($P > 0.05$). Treatment with LM-031 or analogs rescued the reduced p-ERK (from 47% to 100–110%, $P < 0.000$), p-AKT (from 46% to 79–106%, $P = 0.017$ – <0.000) and p-CREB (from 48% to 119–138%, $P < 0.000$) levels, and the rescue was blocked by TRKB-specific shRNA (p-ERK: 56–60%, $P = 0.006$ – <0.001 ; p-AKT: 56–68%, $P = 0.227$ – <0.001 ; p-CREB: 67–91%; $P = 0.037$ – <0.001).

In the aforementioned TRKB-knockdown A β -GFP cells, the effects of LM-031 and analogs on increasing neurite outgrowth were assessed (Figure 5D). Overexpression of A β -GFP resulted in a significant decrease in length (from 30.2 μ m to 22.4 μ m), process (from 4.0 to 2.6), and branch (from 3.1 to 1.8) ($P < 0.001$) of neurite, and shRNA targeting TRKB furthermore decreased neurite length/branch to 18.7 μ m/1.5 ($P = 0.040$ – 0.020). In A β -GFP cells, treatment with the LM-031 or analogs rescued the reduced neurite length (from 22.4 μ m to 27.7–30.9 μ m) and branch (from 1.8 to 2.6–2.9) ($P < 0.001$), and the rescue was blocked by shRNA targeting TRKB (length: 21.9–18.9 μ m, branch: 1.6–1.4; $P < 0.001$). Neurite process was significantly increased only by LM-031 (from 2.6 to 3.8, $P < 0.001$), which was deterred by shRNA targeting TRKB (2.5, $P < 0.001$).

Therapeutic targets of LMDS-1 and -2 in A β -GFP-expressing SH-SY5Y cells

The effects of LMDS-1 and LMDS-2 on expression levels of ERK, AKT and downstream targets of TRKB were examined by applying ERK inhibitor U0126 or PI3K inhibitor wortmannin (10 μ M) to LMDS-1/2-treated SH-SY5Y cells expressing A β -GFP (Figure 6A). Overexpression of A β -GFP down-regulated p-ERK and p-AKT (70–71%, $P = 0.004$ – 0.007), LMDS-1 and -2 treatment rescued the reduction (110–115%, $P < 0.001$), whereas U0126 treatment lowered the elevation of p-ERK (from 115% to 38–43%, $P < 0.001$) and wortmannin treatment lowered the elevation of p-AKT (from 110–111% to 30–29%, $P < 0.001$) (Figure 6B). Additionally, induced expression of A β -GFP reduced p-TRKB Y516 and Y817 (61–64%, $P = 0.004$ – 0.001), p-CREB (66%, $P < 0.001$), pro- and m-BDNF (68–52%, $P = 0.022$ – 0.005) and BCL2 (44%, $P = 0.009$), and increased BCL2 associated X, apoptosis regulator (BAX) (225%, $P = 0.012$). In contrast, treatment with

LMDS-1 and -2 increased p-TRKB Y516 and Y817 (113–123%, $P < 0.001$), p-CREB (127–142%, $P < 0.001$), pro- and m-BDNF (100–169%, $P = 0.025$ –

<0.001) and BCL2 (156–199%, $P < 0.001$), and reduced BAX (121–130%, $P = 0.045$ –0.080). Treatment with U0126 or wortmannin attenuated the increase in

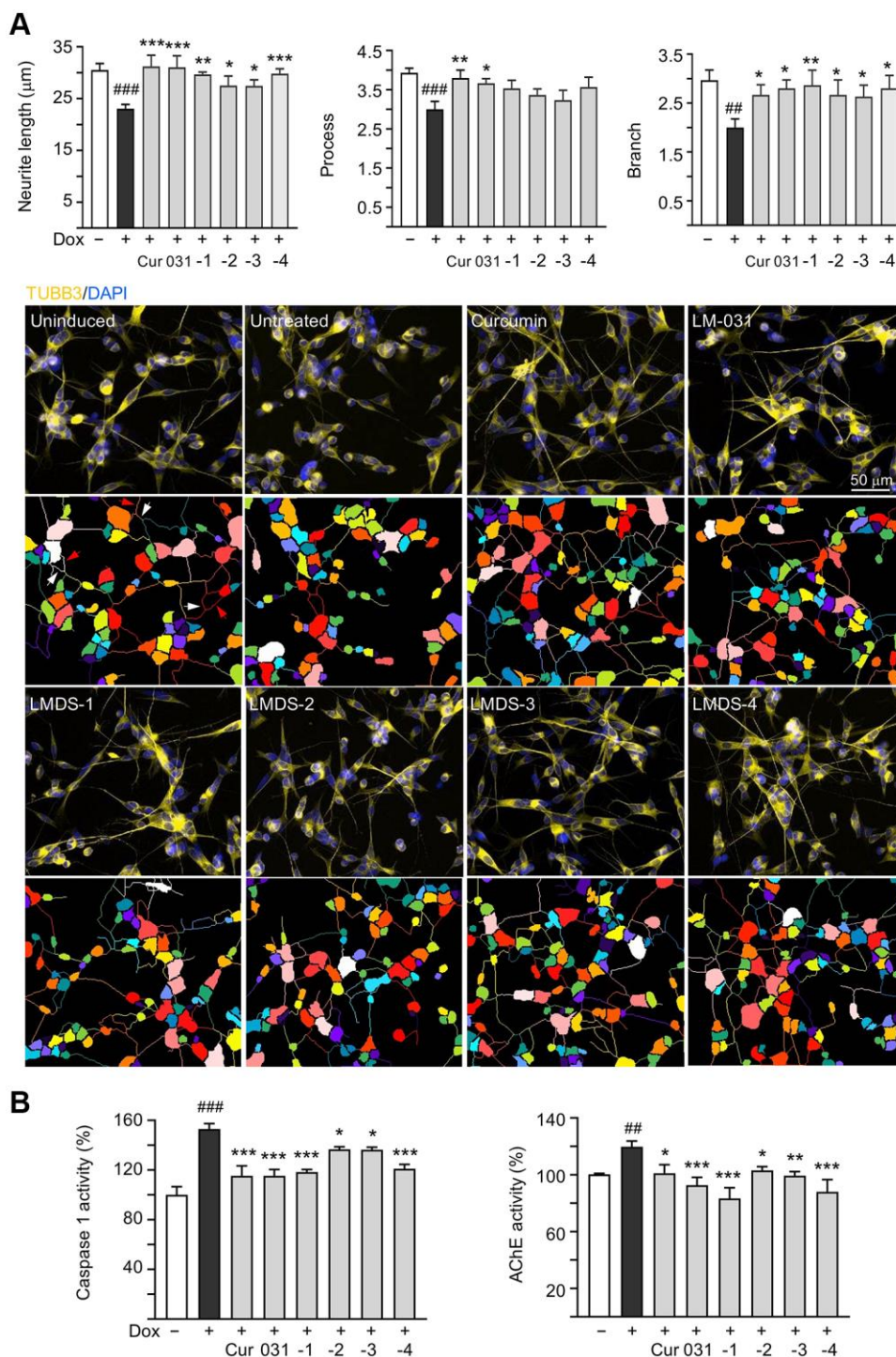


Figure 4. Neuroprotective effects of LM-031 and analogs in Aβ-GFP SH-SY5Y cells. (A) Neurite outgrowth (length, process and branch) assay of Aβ-GFP cells uninduced, untreated, or treated with curcumin, LM-031 or analogs at 5 μM ($n = 3$). Shown below are images of TUBB3 (yellow)-stained cells, with nuclei counterstained with DAPI (blue), and segmented images with multi-colored mask to assign each outgrowth to a cell body for quantification. In uninduced cells, processes and branches are indicated with red and white arrows, respectively. **(B)** Caspase 1 and AChE activity assays with curcumin, LM-031 or analogs (5 μM) treatment ($n = 3$). The relative caspase 1 or AChE activity of uninduced cells (Dox-) was normalized (100%). P values: comparisons between induced (Dox+) vs. uninduced (Dox-) cells ($##P < 0.01$ and $###P < 0.001$), or compound-treated vs. untreated (Dox+) cells ($*P < 0.05$, $**P < 0.01$, $***P < 0.001$). (one-way ANOVA with *post hoc* Tukey test).

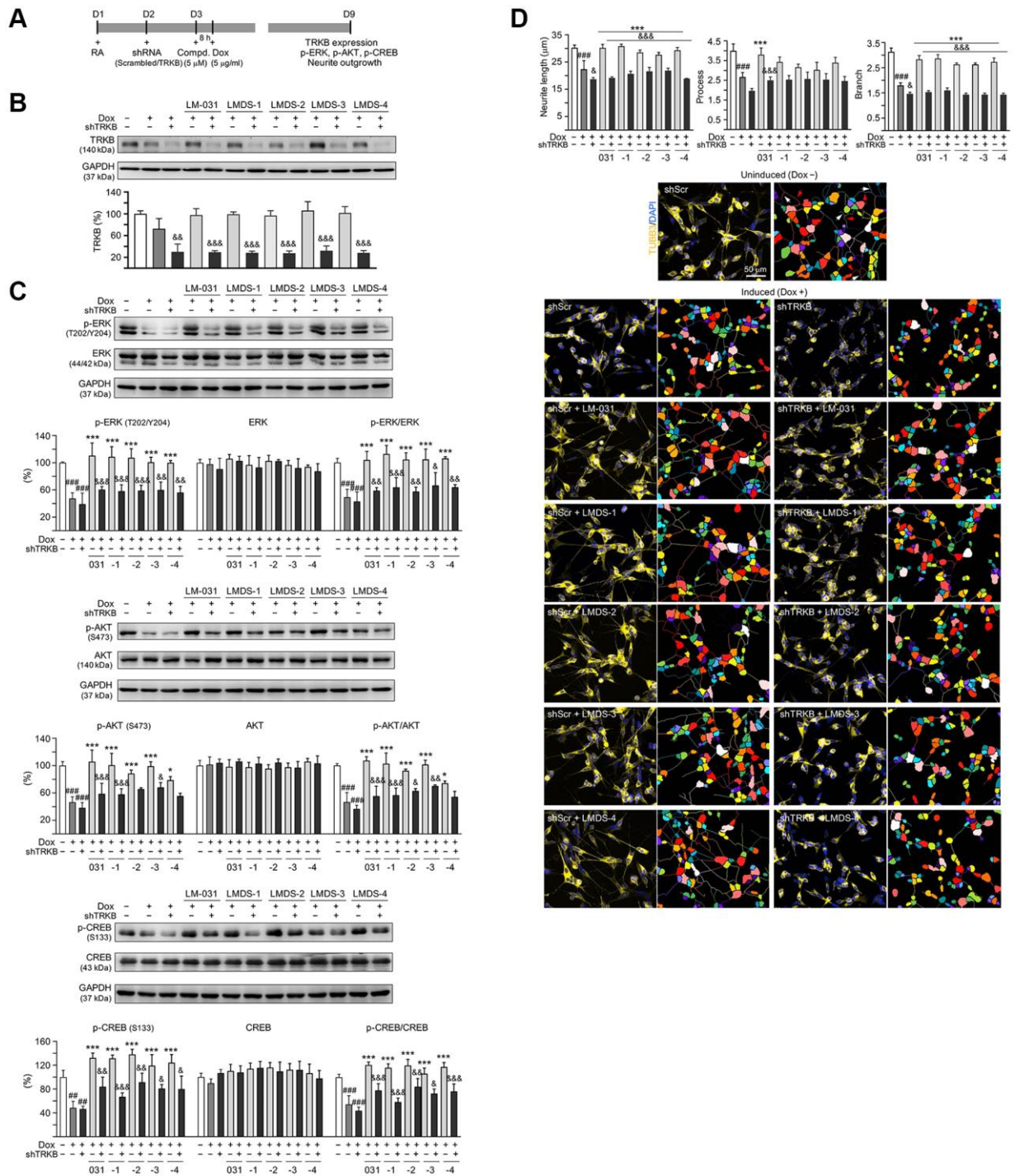


Figure 5. TRKB RNA interference of Aβ-GFP SH-SY5Y cells. (A) Experimental flow chart. On day 1, Aβ-GFP SH-SY5Y cells were plated with retinoic acid (RA; 10 μM). On day 2, the cells were infected with lentivirus-expressing TRKB-specific or scrambled shRNA. At 24 h post-infection, LM-031 or LMDS-1 to -4 (5 μM) was added to the cells for 8 h, followed by induction of Aβ-GFP expression (Dox, 5 μg/ml) for 6 days. On day 9, TRKB and neurite outgrowth analyses were performed. Western blot analysis of (B) TRKB, (C) p-ERK (T202/Y204), ERK, p-AKT (S473), AKT, p-CREB (S133), and CREB in compound-treated cells infected with TRKB-specific or scrambled shRNA-expressing lentivirus ($n = 3$). GAPDH was used as a loading control. To normalize, the relative protein level of uninduced cells was set at 100%. (D) Microscopic images and neurite outgrowth (length, process and branch) assay of Aβ-GFP-expressing cells with TRKB-specific or scrambled shRNA, and with or without LM-031 or analogs (5 μM) treatments ($n = 3$). TUBB3 staining (yellow) was used to quantify the extent of neurite outgrowth. Nuclei were counterstained with DAPI (blue). Also shown were segmented images with multi-colored mask to assign each outgrowth to a cell body for quantification. In uninduced cells, processes and branches are indicated with red and white arrows, respectively. P values: comparisons between induced vs. uninduced cells (### $P < 0.001$), compound-treated vs. untreated (induced) cells (*** $P < 0.001$), or TRKB shRNA-treated vs. scrambled shRNA-treated cells (& $P < 0.05$, && $P < 0.01$, &&& $P < 0.001$). (one-way ANOVA with a *post hoc* Tukey test).

p-CREB (52–84%, $P < 0.001$), pro- and m-BDNF (65–88%, $P = 0.198–<0.001$) and BCL2 (80–121%, $P <$

0.001), and reduced the decrease in BAX (152–191%, $P > 0.05$) (Figure 6C).

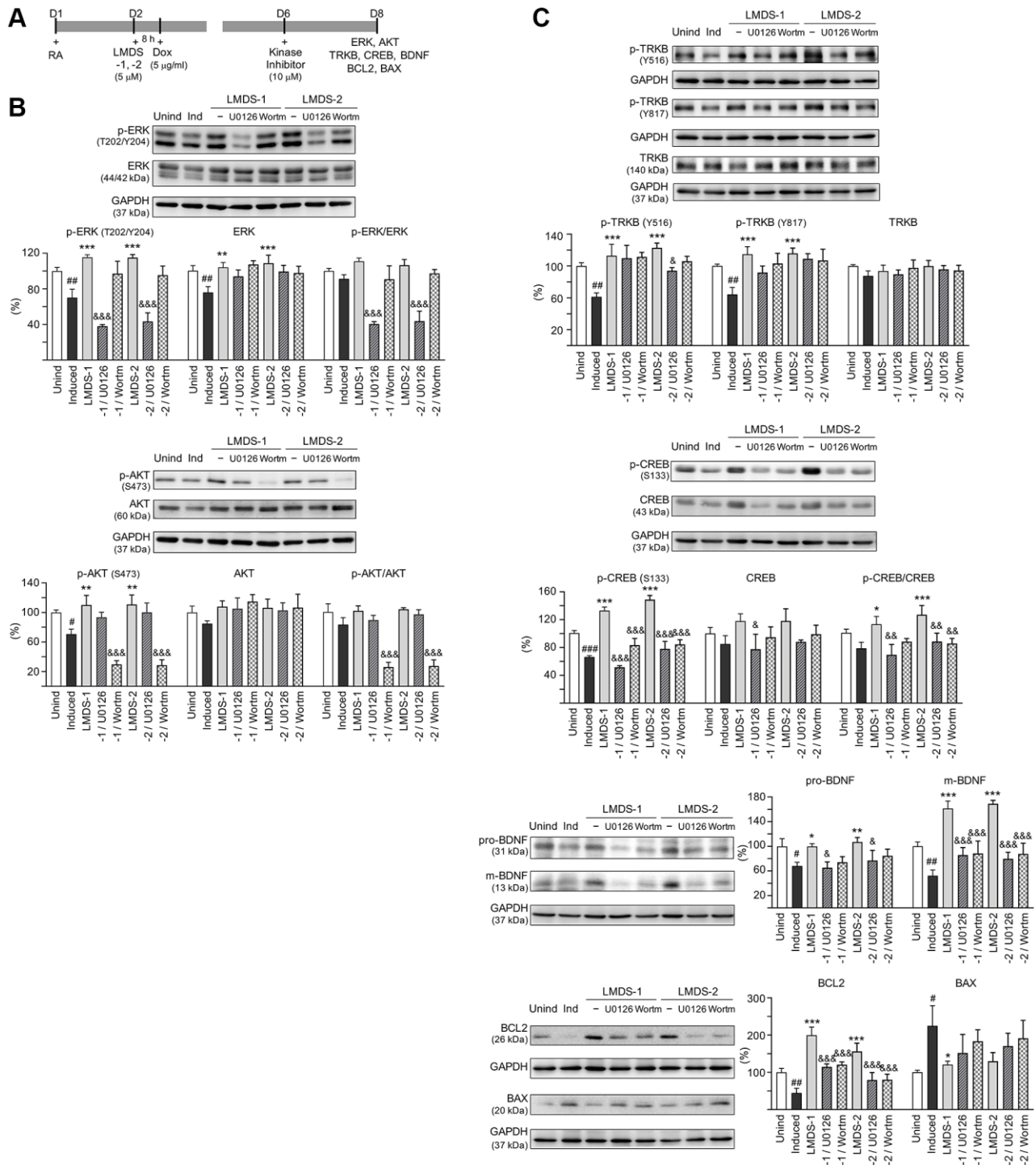


Figure 6. Activation of ERK, AKT and CREB pathways downstream to TRKB in $A\beta$ -GFP SH-SY5Y cells. (A) Experimental flow chart. On day 1, cells were plated with retinoic acid (RA, 10 μ M) into the culture medium. On day 2, LMDS-1 or -2 (5 μ M) was added to the cells for 8 h, followed by inducing $A\beta$ -GFP expression with doxycycline (Dox, 5 μ g/ml). Kinase inhibitors U0126 or wortmannin (10 μ M) were added to the cells on day 6. On day 8, ERK, AKT, TRKB, CREB, BDNF, BCL2 and BAX levels were measured. (B) p-ERK (T202/Y204), ERK, p-AKT (S473), AKT, (C) p-TRKB (Y516 and Y817), TRKB, p-CREB (S133), CREB, BDNF (31/13 kDa), BCL2 and BAX levels analysed by immunoblot using GAPDH as a loading control ($n = 3$). To normalize, protein expression level in untreated cells was set at 100%. P values: comparisons between induced vs. uninduced cells ($\#P < 0.05$, $\##P < 0.01$), compound-treated vs. untreated cells ($*P < 0.05$, $**P < 0.01$, $***P < 0.001$), or kinase inhibitor-treated vs. untreated cells ($\&P < 0.05$, $\&\&P < 0.001$). (one-way ANOVA with a *post hoc* Tukey test).

Comparative effects of LMDS-1, -2 and BDNF on TRKB signaling

As LMDS-1 and -2 target ERK, AKT and downstream CREB, effects of BDNF and LMDS compounds on

TRKB signaling were compared. Oxidative stress attenuation was first evaluated by treating A β -GFP cells with BDNF at 1–100 ng/ml concentration or LMDS-1, -2 at 1.2–5 μ M concentration (Figure 7A). The ROS level induced by A β overexpression was successfully

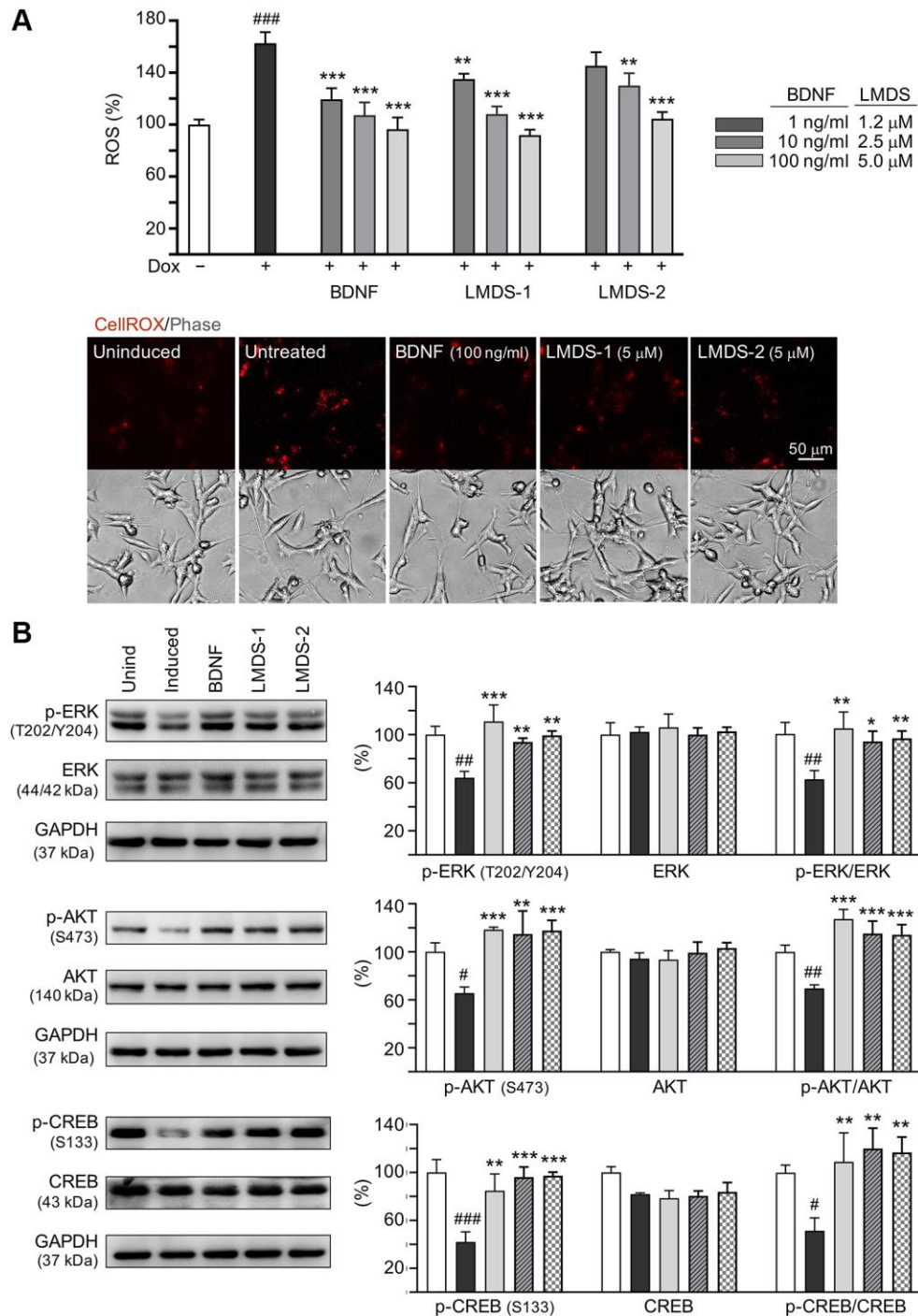


Figure 7. Comparison of BDNF's and LMDS compound's signaling activation. (A) Assessment of ROS in A β -GFP cells uninduced, untreated, treated with treated with BDNF at 1–100 ng/ml, or LMDS-1, -2 at 1.2–5 μ M ($n = 3$). The relative ROS of uninduced cells (Dox-) was normalized (100%). Shown below are images of CellROX[®] Deep Red stain (red). (B) Assessment of p-ERK (T202/Y204), ERK, p-AKT (S473), AKT, p-CREB (S133) and CREB levels with LMDS-1, -2 (5 μ M) or BDNF (100 ng/ml) treatment by immunoblot using GAPDH as a loading control ($n = 3$). To normalize, protein expression level in untreated cells was set at 100%. P values: comparisons between induced vs. uninduced cells ($\#P < 0.05$, $\#\#P < 0.01$), or compound-treated vs. untreated cells ($*P < 0.05$, $**P < 0.01$, $***P < 0.001$). (one-way ANOVA with a *post hoc* Tukey test).

Table 1. Permeability of LM-031, analogs and QC compound by PAMPA-BBB method.

Compound name	Measured P_e (10^{-6} cm/s) or % transport	PAMPA-BBB classification ^a
LM-031	4.80 ± 0.12	BBB ⁺ (high)
LMDS-1	14.88 ± 3.61	BBB ⁺ (high)
LMDS-2	3.81 ± 0.13	BBB ⁺ (moderate)
LMDS-3	11.83 ± 4.11	BBB ⁺ (high)
LMDS-4	–	Not determined (due to low mass recovery)
Bupropion	17.06 ± 1.09	High marker [33]
Piroxicam	1.65 ± 0.17	Low marker [32]
Lucifer yellow	0.00 (% Transport)	Integrity marker

^aSuggested BBB permeability classification: $P_e > 4 \times 10^{-6}$ cm/s (high), $4 > P_e > 2 \times 10^{-6}$ cm/s (moderate), and $P_e < 2 \times 10^{-6}$ cm/s (low).

decreased by BDNF at 1–100 ng/ml, LMDS-1 at 1.2–5 μ M, and LMDS-2 at 2.5–5 μ M (from 163% to 135–92%, $P = 0.007$ – <0.001). BDNF at 100 ng/ml and LMDS-1, -2 at 5 μ M were then selected to compare the efficacy in TRKB signaling (Figure 7B). Overexpression of A β -GFP down-regulated p-ERK (64%, $P = 0.001$), p-AKT (65%, $P = 0.014$) and p-CREB (42%, $P < 0.001$), and BDNF, LMDS-1 and -2 treatment rescued the reduction (p-ERK: 94–111%, $P = 0.005$ – <0.001 ; p-AKT: 115–118%, $P = 0.001$ – <0.001 ; p-CREB: 85–97%, $P = 0.002$ – <0.001). No significant differences in p-ERK, p-AKT and p-CREB were detected between BDNF and LMDS-1/2 groups ($P > 0.05$).

BBB permeability of LM-031 and analogs

As of now, the PAMPA model has been proposed to analyze membrane permeability, including BBB [32, 33]. The *in vitro* BBB permeability of LM-031 and analogs was then estimated using the PAMPA-BBB approach. Quality controls, including high permeability bupropion [33], low permeability piroxicam [32], and integrity marker lucifer yellow, were included for comparison. Bupropion and piroxicam, which represent high ($> 4 \times 10^{-6}$ cm/s) and low ($< 2 \times 10^{-6}$ cm/s) BBB permeable controls, had effective permeability (P_e) values of 17.06 and 1.65 (10^{-6} cm/s), respectively (Table 1). Well-accepted membrane integrity (below the 0.1% cut-off) was demonstrated by the unnoticeable transport of Lucifer yellow. The P_e values of LM-031, LMDS-1, -2 and -3 were 4.80 ± 0.12 [34], 14.88 ± 3.61, 3.81 ± 0.13 and 11.83 ± 4.11 (10^{-6} cm/s) respectively, suggesting to be categorized as BBB permeable ($P_e > 2 \times 10^{-6}$ cm/s) in PAMPA-BBB measurement. Due to the low mass recovery (12.7%), the P_e value of LMDS-4 was not determined.

DISCUSSION

There are several reasons for identifying small molecules acting as novel potential TRKB agonists for

AD therapeutic uses. First, there is no available treatment currently to cure AD or to halt its progression. Second, substantial evidence has shown that decreased BDNF and impaired TRKB pathways, including ERK, CREB and PI3K-AKT, contribute to neurodegeneration in AD [13–17]. Third, agents enhancing BDNF expression or TRKB agonists provide beneficial effects to AD [35–37]. Fourth, BDNF hardly penetrates BBB into brain [21]. Thus, identifying TRKB agonists with good BBB permeability may provide a therapeutic strategy for AD. In the present study, we identified novel potential TRKB agonists with good bioavailability (Figure 1). This is supported by the calculated values of MW, HBD, HBA and cLogP of these compounds because they satisfy the Lipinski's criteria [24]. Furthermore, PSA of less than 90 Å² [25] and predicted BBB scores of greater than threshold 0.02 [26] support a good BBB permeability of these compounds (Figure 1). The binding scores predicted by docking computations suggest these compounds have a good affinity to d5-domain of TRKB (Figure 2), providing evidence of their potential as TRKB agonists.

LM-031 and LMDS-1 to -4 significantly reduced ROS production (Figure 3) and promoted neurite outgrowth (Figure 4) in induced A β -GFP SH-SY5Y cells. TRKB signaling is a key factor regulating neuron survival, differentiation, dendritic and axonal growth and branching, as well synaptic plasticity [38–40]. In addition, TRKB agonist 7,8-DHF displayed anti-oxidative, anti-inflammatory, and anti-apoptotic effects to protect against cerebral injury [41]. Consistent with these previous reports, our results showed that LM-031 and analogs stimulated neurite outgrowth and branching by activating TRKB signaling, and knock-down of TRKB significantly attenuated the neurite outgrowth promoting effects (Figure 5).

In addition to targeting TRKB, neurotrophic receptor tyrosine kinase 1 (TRKA) agonist D3 have been shown to provide beneficial effects to activate TRKA-

related signaling cascades and enhance cholinergic neurotransmission in transgenic mice overexpressing human APP with KM670/671NL and V717F mutations [42]. Targeting neurotrophic receptor tyrosine kinase 3 (TRKC) signaling may also be an effective approach to rescue impaired cholinergic function in AD [43]. Our study results demonstrate that LMDS compounds specific for TRKB binding enhance neurite outgrowth by activating signaling downstream of TRKB. Whether TRK receptor isoforms TRKA and TRKC could potentially be activated by LMDS compounds remains to be determined. In addition, future *in vitro* binding assay should be performed to provide evidence of LMDS compounds binding to extracellular domain of TRKB [22] to show their specificity of TRKB binding.

Once TRKB is activated, three major signaling cascades, PLC- γ 1, ERK and PI3K-AKT, ensue [44]. CREB can be phosphorylated at S133 by both p-ERK and p-AKT, and p-CREB (S133) can further enhance BDNF expression. We examined if LM-031, LMDS-1 and -2 would act on TRKB signaling pathways, including ERK-CREB and PI3K-AKT-CREB. As shown in Figure 6, ERK inhibitor U0126 and PI3K inhibitor wortmannin, respectively, decreased p-CREB and mature BDNF in SH-SY5Y cells expressing A β -GFP, suggesting that LM-031, LMDS-1 and -2 exerted their neuroprotection effects via enhancing PI3K-AKT-CREB and ERK-CREB pathways. CREB phosphorylation up-regulates cAMP responsive element-mediated genes, including BDNF and BCL2, which provides neuroprotective effects against apoptosis [45, 46]. BCL2 was enhanced by LMDS-1 and -2 and BAX reduced by LMDS-1, which effects were diminished by ERK inhibitor or PI3K inhibitor, further implicating that ERK, PI3K-AKT and CREB pathways contribute to neuroprotection in the A β -GFP model.

Several known small molecules or compounds such as catalpol, cystamine, rosmarinic acid and wogonin could increase BDNF expression, but their role as TRKB agonists are not validated [47–50]. Up to now, a few TRKB agonists have been developed to treat neurodegenerative models. Among them, 7,8-DHF demonstrates the features of a potent TRKB agonist and the effects of preventing A β deposition, deficits of hippocampal synapses and memory impairment in 5 \times FAD (APP K670N, M671L, I716V and V717I mutations along with PS1 M146L and L286V mutations) [51] or Tg2576 (APP K670N and M671L mutations) [52] AD mice. 7,8-DHF also elevates cellular glutathione levels and diminishes ROS stress caused by glutamate in HT-22 cells [53] and protects PC12 cells from cytotoxicity induced by 6-

hydroxydopamine through increasing superoxide dismutase and decreasing malondialdehyde [54]. It also suppresses the accumulation of α -synuclein and oxidative stress via activating TRKB [55]. Similar to 7,8-DHF, the LMDS-1 and -2 also significantly reduced oxidative stress in A β -GFP cells. 7,8-DHF has a high affinity with TRKB [56, 57]. LM22A-4 is also a TRKB agonist, which has shown TRKB-activating and neurodegeneration-preventing effects in rodents, but LM22A-4 has a poor BBB penetration ability [58]. Similar to 7,8-DHF, LMDS-1 and -2, respectively displayed a good BBB permeability as shown by PAMPA-BBB measurement (Table 1), suggesting their potentials to treat neurodegenerative diseases. Application of LMDS-1 and -2 to animal models are warranted to confirm the neuroprotection effects.

CONCLUSIONS

In this study, we identified LM-031 analogous compounds LMDS-1 and -2 which may serve as the potential TRKB agonists to treat AD. This is supported by our experimental results demonstrating TRKB signaling-activating, aggregation-inhibitory, oxidative stress- and caspase 1-reducing, and neurite outgrowth-promoting effects in A β -GFP SH-SY5Y cells. Pursuit of analogous compounds resembled to the identified compounds should be of interest in the future.

MATERIALS AND METHODS

Test compounds and BDNF

In-house LM-031 activating the CREB-dependent survival and anti-apoptosis pathway was prepared as described [23]. To search for LM-031 analogous compounds, InterBioScreen Ltd. (<https://www.ibscreen.com/>), ChEMBL (<https://www.ebi.ac.uk/chembl/>) and ZINC (<http://zinc15.docking.org/>) databases were screened using compound similarity search software tools. Four top-scoring compounds LMDS-1 to -4 were selected and obtained from Enamine (Kyiv, Ukraine). In cell culture media, these five compounds had no solubility problems all the way to 100 μ M. The following items were bought from Sigma-Aldrich Co. (St. Louis, MO, USA): curcumin (control for monitoring A β folding), kaempferol (antioxidant control in DPPH assay), coumarin (backbone of LM-031 and analogs) and BDNF.

Bioavailability and BBB permeation prediction

Using Internet software ChemDraw (<http://www.perkinelmer.com/tw/category/chemdraw/>), the following properties of LM-031 and its analogs were computed: MW, HBD, HBA, cLogP, and PSA.

Additionally, BBB permeation scores were derived utilizing the BBB prediction server Online BBB Predictor (<https://www.cbiligand.org/BBB/>) [26].

Anti-amyloid and antioxidant assays

Thioflavin T is widely used to visualize and quantify the presence of misfolded amyloid protein aggregates *in vitro* [59]. The A β amyloid inhibiting potential of curcumin, LM-031 and analogs (5–20 μ M) were assessed by using A β 42 peptide (AnaSpec, Fremont, CA, USA) upon binding to thioflavin T as stated [60]. In addition, DPPH radical (Sigma-Aldrich) [61] was used to assay the free radical scavenging capacity of kaempferol, LM-031 and analogs (10–160 μ M) as stated [60].

Docking computation

Docking calculations for LM-031 and analogs were carried out using the GOLD docking program [62, 63]. The computational protocol was similar to our previous study [64]. Briefly, protein structure of domain d5 of TRKB (pdb code: 1HCF) [65] was used for docking compounds. The d5 domain determined the specificity of neurotrophin receptors experimentally [66]. Binding site of small molecule agonists has been predicted by a previous computation [67]. To assure convergence of the computed findings, the numbers of operations of 10,000, 20,000, 40,000 and 80,000 were carried out in the current docking computations of LM-031 and analogs. For comparison, 7,8-DHF, a bioactive TRKB agonist [22], was also added to the computation.

Cells and culture

Human neuroblastoma SH-SY5Y-derived A β -GFP cells were maintained as stated [29]. The recombinant A β -GFP protein has a 12 amino acid-containing linker between the fused A β and GFP. Doxycycline (5 μ g/ml; Sigma-Aldrich) was used to induce A β -GFP expression.

A β folding reporter fluorescence and oxidative stress analyses

Neuronal differentiation of A β -GFP SH-SY5Y cells was induced by retinoic acid (10 μ M; Sigma-Aldrich) [68]. Cells on 96-well plate (2.5×10^4 /well) were seeded on day 1, pre-treated with test compounds (1.2–5 μ M) plus induced A β -GFP expression (5 μ g/ml doxycycline) on day 2, and stained with Hoechst 33342 (0.1 μ g/ml; Sigma-Aldrich) on day 8 as stated [60]. Cell images were then captured at 482 nm excitation/536 nm emission wavelengths (ImageXpress Micro Confocal high-content system) and analyzed (MetaXpress image acquisition and analysis software) (Molecular Devices,

Sunnyvale, CA, USA). In addition, ROS was quantified on day 8 following CellROX Deep Red stain (5 μ M; Molecular Probes, Waltham, MA, USA) using the high-content system with excitation/emission wavelengths of 644/665 nm.

Real-time PCR analysis

Total RNA was extracted, converted to cDNA, and the expressed A β -GFP RNA was quantified as stated [69]. The formula $2^{\Delta\Delta C_t}$, $\Delta\Delta C_t = C_T$ (HPRT1) - C_T (EGFP), where C_T stands for cycle threshold, was used to compute fold change.

Neurite outgrowth analysis

As stated, A β -GFP SH-SY5Y cells were seeded (6×10^4 /24-well) with retinoic acid addition on day 1, treated with tested compounds (5 μ M) plus induced A β -GFP expression (5 μ g/ml doxycycline) on day 2, and stained with TUBB3 (tubulin beta 3 class III) primary antibody (1:1000; Covance #MMS-435P, Princeton, NJ, USA), goat anti-rabbit Alexa Fluor[®] 555 secondary antibody (1:1000; Thermo Fisher Scientific #A27039), and DAPI (4'-6-diamidino-2-phenylindole, 0.1 μ g/ml; Sigma-Aldrich) on day 8 [60]. Neuronal pictures were taken using the high-content system and analyzed for neurite length (μ m), process (number of neurites protruding from neuronal cell body) and branch (number of neurites extending from process) (MetaXpress neurite outgrowth application module; Molecular Devices). In each of three independent experiments, roughly 6000 cells from each sample were examined.

Caspase 1 and AChE activity assays

Cells on 6-well plate (5×10^5 /well) were subjected to the retinoic acid, test compound and doxycycline treatments as stated. Cells were collected on day 8 and cell lysates prepared for caspase 1 (BioVision, Milpitas, CA, USA) and AChE (Sigma-Aldrich) activity measurement [60].

TRKB RNA interference

To knock down TRKB expression in A β -GFP SH-SY5Y cells, lentiviral short hairpin RNA (shRNA) targeting TRKB and control (scrambled) were used [69]. Cells were plated in the presence of retinoic acid (5×10^5 /6-well for protein analysis or 6×10^4 /24-well for neurite outgrowth analysis) on day 1, infected with lentivirus on day 2, pretreated with test compound (5 μ M) plus inducing A β -GFP expression on day 3, and collected for neurite outgrowth or TRKB protein analysis on day 9 as stated [69].

ERK/PI3K kinase inhibitor treatment

Cells were plated in the presence of retinoic acid ($5 \times 10^5/6$ -well) on day 1, treated with tested compounds ($5 \mu\text{M}$) plus induced A β -GFP expression with doxycycline ($5 \mu\text{g/ml}$) on day 2, as stated. Kinase inhibitors U0126 (an inhibitor of ERK) or wortmannin (an inhibitor of PI3K) (LC Laboratories, Woburn, MA, USA) ($10 \mu\text{M}$) were added on day 6. The cells were collected on day 8 for BDNF, BCL2, BAX, total/phosphorylated TRKB, ERK, AKT, and CREB protein analysis as previously stated.

Immunoblot analysis

Total proteins from A β -GFP SH-SY5Y cells were prepared, quantified, electrophoretically separated and blotted as stated [60]. Following blocking, the membrane was probed with antibody against BDNF (1:500; Santa Cruz Biotechnology #sc-546, Santa Cruz, CA, USA), BCL2 (1:200; Santa Cruz Biotechnology #sc-7382), BAX (1:200; Santa Cruz Biotechnology #sc-7480), TRKB (1:500; Cell Signaling Technology #4603, Danvers, MA, USA), p-TRKB (Y516) (1:200; GeneTex #GTX32230, Irvine, CA, USA), p-TRKB (Y816) (1:1000; Millipore #ABN1381, Billerica, MA, USA), ERK (1:1000; Cell Signaling Technology #9102), p-ERK (T202/Y204) (1:1000; Cell Signaling Technology #9101), AKT (1:1000; Abcam #ab126811, Cambridge, CB, UK), p-AKT (S473) (1:1000; Cell Signaling Technology #4060), CREB (1:500; Santa Cruz Biotechnology #sc-186), p-CREB (S133) (1:1000; Millipore #06-519), or loading control GAPDH (glyceraldehyde-3-phosphate dehydrogenase) (1:1000; MDBio #30000002, Taipei, Taiwan). The immune complexes were detected as stated [60].

PAMPA to assess BBB permeability

The permeability of LMDS-1 and -2 was determined by a PAMPA-BBB assay. Firstly, $300 \mu\text{l}$ of LMDS-1 or -2 ($1 \mu\text{M}$) solution were added to the donor well (Millipore). Bupropion (a high permeability marker), piroxicam (a low permeability marker), and lucifer yellow (an integrity marker) (Sigma-Aldrich) were used as quality control (QC) compounds for comparison. The sandwich with aqueous donor on the bottom, artificial lipid membrane (PVDF filter coated with porcine polar brain lipid) in the middle, and aqueous acceptor (5% DMSO in PBS) on the top was assembled as stated [69]. Each compound was tested in triplicate. After incubation for 18 h at the ambient temperature, the PAMPA sandwich plate was separated. The concentrations of test and QC compounds in the donor and acceptor wells were measured as stated [69], and the effective permeability coefficient (P_e) was computed [70].

Statistical analysis

The mean \pm standard deviation from three independent experiments are reported as the data. As appropriate, a two-tailed Student's *t* test or one-way ANOVA (analysis of variance) with a *post hoc* Tukey test were used to assess group differences. *P* values < 0.05 indicated statistical significance.

AUTHOR CONTRIBUTIONS

Conception and design: CMC, YCS, and GJLC; Experiments conduction and data acquisition: YJC, THL; Data analysis: YJC, THL, GJLC; Drafting of the manuscript: CMC, GJLC; Contributed reagents/materials: KHC, WL, HMHL, MTS; Critical revision of manuscript: CMC, YCS, and GJLC; Final approval of manuscript: CMC, GJLC.

ACKNOWLEDGMENTS

We thank the Molecular Imaging Core Facility of National Taiwan Normal University for the technical assistance. We also thank the National RNAi Core Facility, Academia Sinica, for technical support. The National Center for High-performance Computing is acknowledged for providing computational resource for docking computation.

CONFLICTS OF INTEREST

The authors declare no conflicts of interest related to this study.

FUNDING

This work was supported by the grants 109-2320-B-003-008, 109-2320-B-182A-021 and 109-2811-B-003-503 from the Ministry of Science and Technology, Taiwan.

REFERENCES

1. Goedert M, Sisodia SS, Price DL. Neurofibrillary tangles and beta-amyloid deposits in Alzheimer's disease. *Curr Opin Neurobiol.* 1991; 1:441–7. [https://doi.org/10.1016/0959-4388\(91\)90067-h](https://doi.org/10.1016/0959-4388(91)90067-h) PMID:1821689
2. Hardy J. Amyloid, the presenilins and Alzheimer's disease. *Trends Neurosci.* 1997; 20:154–9. [https://doi.org/10.1016/s0166-2236\(96\)01030-2](https://doi.org/10.1016/s0166-2236(96)01030-2) PMID:9106355
3. Hardy J, Allsop D. Amyloid deposition as the central event in the aetiology of Alzheimer's disease. *Trends Pharmacol Sci.* 1991; 12:383–8.

- [https://doi.org/10.1016/0165-6147\(91\)90609-v](https://doi.org/10.1016/0165-6147(91)90609-v)
PMID:[1763432](https://pubmed.ncbi.nlm.nih.gov/1763432/)
4. Roher AE, Lowenson JD, Clarke S, Woods AS, Cotter RJ, Gowing E, Ball MJ. beta-Amyloid-(1-42) is a major component of cerebrovascular amyloid deposits: implications for the pathology of Alzheimer disease. *Proc Natl Acad Sci U S A*. 1993; 90:10836–40.
<https://doi.org/10.1073/pnas.90.22.10836>
PMID:[8248178](https://pubmed.ncbi.nlm.nih.gov/8248178/)
 5. Koo EH, Lansbury PT Jr, Kelly JW. Amyloid diseases: abnormal protein aggregation in neurodegeneration. *Proc Natl Acad Sci U S A*. 1999; 96:9989–90.
<https://doi.org/10.1073/pnas.96.18.9989>
PMID:[10468546](https://pubmed.ncbi.nlm.nih.gov/10468546/)
 6. Small DH, Mok SS, Bornstein JC. Alzheimer's disease and Abeta toxicity: from top to bottom. *Nat Rev Neurosci*. 2001; 2:595–8.
<https://doi.org/10.1038/35086072>
PMID:[11484003](https://pubmed.ncbi.nlm.nih.gov/11484003/)
 7. Butterfield DA, Swomley AM, Sultana R. Amyloid β -peptide (1-42)-induced oxidative stress in Alzheimer disease: importance in disease pathogenesis and progression. *Antioxid Redox Signal*. 2013; 19:823–35.
<https://doi.org/10.1089/ars.2012.5027>
PMID:[23249141](https://pubmed.ncbi.nlm.nih.gov/23249141/)
 8. Liu L, Chan C. The role of inflammasome in Alzheimer's disease. *Ageing Res Rev*. 2014; 15:6–15.
<https://doi.org/10.1016/j.arr.2013.12.007>
PMID:[24561250](https://pubmed.ncbi.nlm.nih.gov/24561250/)
 9. Lu B, Nagappan G, Guan X, Nathan PJ, Wren P. BDNF-based synaptic repair as a disease-modifying strategy for neurodegenerative diseases. *Nat Rev Neurosci*. 2013; 14:401–16.
<https://doi.org/10.1038/nrn3505>
PMID:[23674053](https://pubmed.ncbi.nlm.nih.gov/23674053/)
 10. Islam O, Loo TX, Heese K. Brain-derived neurotrophic factor (BDNF) has proliferative effects on neural stem cells through the truncated TRK-B receptor, MAP kinase, AKT, and STAT-3 signaling pathways. *Curr Neurovasc Res*. 2009; 6:42–53.
<https://doi.org/10.2174/156720209787466028>
PMID:[19355925](https://pubmed.ncbi.nlm.nih.gov/19355925/)
 11. Murray PS, Holmes PV. An overview of brain-derived neurotrophic factor and implications for excitotoxic vulnerability in the hippocampus. *Int J Pept*. 2011; 2011:654085.
<https://doi.org/10.1155/2011/654085>
PMID:[21966294](https://pubmed.ncbi.nlm.nih.gov/21966294/)
 12. Zuccato C, Cattaneo E. Brain-derived neurotrophic factor in neurodegenerative diseases. *Nat Rev Neurol*. 2009; 5:311–22.
<https://doi.org/10.1038/nrneurol.2009.54>
PMID:[19498435](https://pubmed.ncbi.nlm.nih.gov/19498435/)
 13. Phillips HS, Hains JM, Armanini M, Laramée GR, Johnson SA, Winslow JW. BDNF mRNA is decreased in the hippocampus of individuals with Alzheimer's disease. *Neuron*. 1991; 7:695–702.
[https://doi.org/10.1016/0896-6273\(91\)90273-3](https://doi.org/10.1016/0896-6273(91)90273-3)
PMID:[1742020](https://pubmed.ncbi.nlm.nih.gov/1742020/)
 14. Peng S, Wu J, Mufson EJ, Fahnstock M. Precursor form of brain-derived neurotrophic factor and mature brain-derived neurotrophic factor are decreased in the pre-clinical stages of Alzheimer's disease. *J Neurochem*. 2005; 93:1412–21.
<https://doi.org/10.1111/j.1471-4159.2005.03135.x>
PMID:[15935057](https://pubmed.ncbi.nlm.nih.gov/15935057/)
 15. Rosa E, Fahnstock M. CREB expression mediates amyloid β -induced basal BDNF downregulation. *Neurobiol Aging*. 2015; 36:2406–13.
<https://doi.org/10.1016/j.neurobiolaging.2015.04.014>
PMID:[26025137](https://pubmed.ncbi.nlm.nih.gov/26025137/)
 16. Vitolo OV, Sant'Angelo A, Costanzo V, Battaglia F, Arancio O, Shelanski M. Amyloid beta -peptide inhibition of the PKA/CREB pathway and long-term potentiation: reversibility by drugs that enhance cAMP signaling. *Proc Natl Acad Sci U S A*. 2002; 99:13217–21.
<https://doi.org/10.1073/pnas.172504199>
PMID:[12244210](https://pubmed.ncbi.nlm.nih.gov/12244210/)
 17. Tong L, Balazs R, Thornton PL, Cotman CW. Beta-amyloid peptide at sublethal concentrations downregulates brain-derived neurotrophic factor functions in cultured cortical neurons. *J Neurosci*. 2004; 24:6799–809.
<https://doi.org/10.1523/JNEUROSCI.5463-03.2004>
PMID:[15282285](https://pubmed.ncbi.nlm.nih.gov/15282285/)
 18. Han K, Jia N, Li J, Yang L, Min LQ. Chronic caffeine treatment reverses memory impairment and the expression of brain BDNF and TrkB in the PS1/APP double transgenic mouse model of Alzheimer's disease. *Mol Med Rep*. 2013; 8:737–40.
<https://doi.org/10.3892/mmr.2013.1601>
PMID:[23900282](https://pubmed.ncbi.nlm.nih.gov/23900282/)
 19. Fukumoto K, Mizoguchi H, Takeuchi H, Horiuchi H, Kawanokuchi J, Jin S, Mizuno T, Suzumura A. Fingolimod increases brain-derived neurotrophic factor levels and ameliorates amyloid β -induced memory impairment. *Behav Brain Res*. 2014; 268:88–93.
<https://doi.org/10.1016/j.bbr.2014.03.046>
PMID:[24713151](https://pubmed.ncbi.nlm.nih.gov/24713151/)
 20. Shin MK, Kim HG, Baek SH, Jung WR, Park DI, Park JS, Jo DG, Kim KL. Neuropep-1 ameliorates learning and memory deficits in an Alzheimer's disease mouse

- model, increases brain-derived neurotrophic factor expression in the brain, and causes reduction of amyloid beta plaques. *Neurobiol Aging*. 2014; 35:990–1001.
<https://doi.org/10.1016/j.neurobiolaging.2013.10.091>
PMID:24268884
21. Dittrich F, Ochs G, Grosse-Wilde A, Berweiler U, Yan Q, Miller JA, Toyka KV, Sendtner M. Pharmacokinetics of intrathecally applied BDNF and effects on spinal motoneurons. *Exp Neurol*. 1996; 141:225–39.
<https://doi.org/10.1006/exnr.1996.0157>
PMID:8812156
22. Jang SW, Liu X, Yepes M, Shepherd KR, Miller GW, Liu Y, Wilson WD, Xiao G, Blanchi B, Sun YE, Ye K. A selective TrkB agonist with potent neurotrophic activities by 7,8-dihydroxyflavone. *Proc Natl Acad Sci U S A*. 2010; 107:2687–92.
<https://doi.org/10.1073/pnas.0913572107>
PMID:20133810
23. Lee SY, Chiu YJ, Yang SM, Chen CM, Huang CC, Lee-Chen GJ, Lin W, Chang KH. Novel synthetic chalcone-coumarin hybrid for A β aggregation reduction, antioxidation, and neuroprotection. *CNS Neurosci Ther*. 2018; 24:1286–98.
<https://doi.org/10.1111/cns.13058>
PMID:30596401
24. Lipinski CA, Lombardo F, Dominy BW, Feeney PJ. Experimental and computational approaches to estimate solubility and permeability in drug discovery and development settings. *Adv Drug Deliv Rev*. 2001; 46:3–26.
[https://doi.org/10.1016/s0169-409x\(00\)00129-0](https://doi.org/10.1016/s0169-409x(00)00129-0)
PMID:11259830
25. Hitchcock SA, Pennington LD. Structure-brain exposure relationships. *J Med Chem*. 2006; 49:7559–83.
<https://doi.org/10.1021/jm060642i>
PMID:17181137
26. Liu H, Wang L, Lv M, Pei R, Li P, Pei Z, Wang Y, Su W, Xie XQ. AlzPlatform: an Alzheimer's disease domain-specific chemogenomics knowledgebase for polypharmacology and target identification research. *J Chem Inf Model*. 2014; 54:1050–60.
<https://doi.org/10.1021/ci500004h>
PMID:24597646
27. Yang F, Lim GP, Begum AN, Ubeda OJ, Simmons MR, Ambegaokar SS, Chen PP, Kaye R, Glabe CG, Frautschy SA, Cole GM. Curcumin inhibits formation of amyloid beta oligomers and fibrils, binds plaques, and reduces amyloid in vivo. *J Biol Chem*. 2005; 280:5892–901.
<https://doi.org/10.1074/jbc.M404751200>
PMID:15590663
28. Zuk M, Kulma A, Dymińska L, Szołtysek K, Prescha A, Hanuza J, Szopa J. Flavonoid engineering of flax potentiate its biotechnological application. *BMC Biotechnol*. 2011; 11:10.
<https://doi.org/10.1186/1472-6750-11-10>
PMID:21276227
29. Chang KH, Chiu YJ, Chen SL, Huang CH, Lin CH, Lin TH, Lee CM, Ramesh C, Wu CH, Huang CC, Fung HC, Chen YC, Lin JY, et al. The potential of synthetic indolylquinoline derivatives for A β aggregation reduction by chemical chaperone activity. *Neuropharmacology*. 2016; 101:309–19.
<https://doi.org/10.1016/j.neuropharm.2015.09.005>
PMID:26362358
30. Zhao T, Zeng Y, Kermod AR. A plant cell-based system that predicts a β 42 misfolding: potential as a drug discovery tool for Alzheimer's disease. *Mol Genet Metab*. 2012; 107:571–9.
<https://doi.org/10.1016/j.ymgme.2012.08.010>
PMID:22944366
31. Thapa A, Jett SD, Chi EY. Curcumin Attenuates Amyloid- β Aggregate Toxicity and Modulates Amyloid- β Aggregation Pathway. *ACS Chem Neurosci*. 2016; 7:56–68.
<https://doi.org/10.1021/acschemneuro.5b00214>
PMID:26529184
32. Di L, Kerns EH, Fan K, McConnell OJ, Carter GT. High throughput artificial membrane permeability assay for blood-brain barrier. *Eur J Med Chem*. 2003; 38:223–32.
[https://doi.org/10.1016/s0223-5234\(03\)00012-6](https://doi.org/10.1016/s0223-5234(03)00012-6)
PMID:12667689
33. Di L, Kerns EH, Bezar IF, Petusky SL, Huang Y. Comparison of blood-brain barrier permeability assays: in situ brain perfusion, MDR1-MDCKII and PAMPA-BBB. *J Pharm Sci*. 2009; 98:1980–91.
<https://doi.org/10.1002/jps.21580>
PMID:18837012
34. Lin TH, Chiu YJ, Lin CH, Lin CY, Chao CY, Chen YC, Yang SM, Lin W, Mei Hsieh-Li H, Wu YR, Chang KH, Lee-Chen GJ, Chen CM. Exploration of multi-target effects of 3-benzoyl-5-hydroxychromen-2-one in Alzheimer's disease cell and mouse models. *Aging Cell*. 2020; 19:e13169.
<https://doi.org/10.1111/acer.13169>
PMID:32496635
35. Nagahara AH, Mateling M, Kovacs I, Wang L, Eggert S, Rockenstein E, Koo EH, Masliah E, Tuszynski MH. Early BDNF treatment ameliorates cell loss in the entorhinal cortex of APP transgenic mice. *J Neurosci*. 2013; 33:15596–602.
<https://doi.org/10.1523/JNEUROSCI.5195-12.2013>
PMID:24068826

36. Jiao SS, Shen LL, Zhu C, Bu XL, Liu YH, Liu CH, Yao XQ, Zhang LL, Zhou HD, Walker DG, Tan J, Götz J, Zhou XF, Wang YJ. Brain-derived neurotrophic factor protects against tau-related neurodegeneration of Alzheimer's disease. *Transl Psychiatry*. 2016; 6:e907.
<https://doi.org/10.1038/tp.2016.186>
PMID:27701410
37. Eremenko E, Mittal K, Berner O, Kamenetsky N, Nemirovsky A, Elyahu Y, Monsonogo A. BDNF-producing, amyloid β -specific CD4 T cells as targeted drug-delivery vehicles in Alzheimer's disease. *EBioMedicine*. 2019; 43:424–34.
<https://doi.org/10.1016/j.ebiom.2019.04.019>
PMID:31085101
38. Park H, Poo MM. Neurotrophin regulation of neural circuit development and function. *Nat Rev Neurosci*. 2013; 14:7–23.
<https://doi.org/10.1038/nrn3379>
PMID:23254191
39. Sala C, Segal M. Dendritic spines: the locus of structural and functional plasticity. *Physiol Rev*. 2014; 94:141–88.
<https://doi.org/10.1152/physrev.00012.2013>
PMID:24382885
40. Yan Y, Eipper BA, Mains RE. Kalirin is required for BDNF-TrkB stimulated neurite outgrowth and branching. *Neuropharmacology*. 2016; 107:227–38.
<https://doi.org/10.1016/j.neuropharm.2016.03.050>
PMID:27036892
41. Wang B, Wu N, Liang F, Zhang S, Ni W, Cao Y, Xia D, Xi H. 7,8-dihydroxyflavone, a small-molecule tropomyosin-related kinase B (TrkB) agonist, attenuates cerebral ischemia and reperfusion injury in rats. *J Mol Histol*. 2014; 45:129–40.
<https://doi.org/10.1007/s10735-013-9539-y>
PMID:24045895
42. Xhima K, Markham-Coultres K, Nedev H, Heinen S, Saragovi HU, Hynynen K, Aubert I. Focused ultrasound delivery of a selective TrkA agonist rescues cholinergic function in a mouse model of Alzheimer's disease. *Sci Adv*. 2020; 6:eaax6646.
<https://doi.org/10.1126/sciadv.aax6646>
PMID:32010781
43. Gonzalez S, McHugh TLM, Yang T, Syriani W, Massa SM, Longo FM, Simmons DA. Small molecule modulation of TrkB and TrkC neurotrophin receptors prevents cholinergic neuron atrophy in an Alzheimer's disease mouse model at an advanced pathological stage. *Neurobiol Dis*. 2022; 162:105563.
<https://doi.org/10.1016/j.nbd.2021.105563>
PMID:34838668
44. Numakawa T, Suzuki S, Kumamaru E, Adachi N, Richards M, Kunugi H. BDNF function and intracellular signaling in neurons. *Histol Histopathol*. 2010; 25:237–58.
<https://doi.org/10.14670/HH-25.237>
PMID:20017110
45. Cheng CY, Lin JG, Tang NY, Kao ST, Hsieh CL. Electroacupuncture at different frequencies (5Hz and 25Hz) ameliorates cerebral ischemia-reperfusion injury in rats: possible involvement of p38 MAPK-mediated anti-apoptotic signaling pathways. *BMC Complement Altern Med*. 2015; 15:241.
<https://doi.org/10.1186/s12906-015-0752-y>
PMID:26187498
46. Huang CY, Liou YF, Chung SY, Lin WY, Jong GP, Kuo CH, Tsai FJ, Cheng YC, Cheng FC, Lin JY. Role of ERK signaling in the neuroprotective efficacy of magnesium sulfate treatment during focal cerebral ischemia in the gerbil cortex. *Chin J Physiol*. 2010; 53:299–309.
<https://doi.org/10.4077/cjp.2010.amk063>
PMID:21793341
47. Wang JM, Yang LH, Zhang YY, Niu CL, Cui Y, Feng WS, Wang GF. BDNF and COX-2 participate in anti-depressive mechanisms of catalpol in rats undergoing chronic unpredictable mild stress. *Physiol Behav*. 2015; 151:360–8.
<https://doi.org/10.1016/j.physbeh.2015.08.008>
PMID:26255123
48. Pillai A, Veeranan-Karmegam R, Dhandapani KM, Mahadik SP. Cystamine prevents haloperidol-induced decrease of BDNF/TrkB signaling in mouse frontal cortex. *J Neurochem*. 2008; 107:941–51.
<https://doi.org/10.1111/j.1471-4159.2008.05665.x>
PMID:18786174
49. Fonteles AA, de Souza CM, de Sousa Neves JC, Menezes AP, Santos do Carmo MR, Fernandes FD, de Araújo PR, de Andrade GM. Rosmarinic acid prevents against memory deficits in ischemic mice. *Behav Brain Res*. 2016; 297:91–103.
<https://doi.org/10.1016/j.bbr.2015.09.029>
PMID:26456521
50. Lee B, Sur B, Cho SG, Yeom M, Shim I, Lee H, Hahm DH. Wogonin Attenuates Hippocampal Neuronal Loss and Cognitive Dysfunction in Trimethyltin-Intoxicated Rats. *Biomol Ther (Seoul)*. 2016; 24:328–37.
<https://doi.org/10.4062/biomolther.2015.152>
PMID:27133262
51. Zhang Z, Liu X, Schroeder JP, Chan CB, Song M, Yu SP, Weinschenker D, Ye K. 7,8-dihydroxyflavone prevents synaptic loss and memory deficits in a mouse model of Alzheimer's disease. *Neuropsychopharmacology*. 2014; 39:638–50.

- <https://doi.org/10.1038/npp.2013.243>
PMID:24022672
52. Gao L, Tian M, Zhao HY, Xu QQ, Huang YM, Si QC, Tian Q, Wu QM, Hu XM, Sun LB, McClintock SM, Zeng Y. TrkB activation by 7, 8-dihydroxyflavone increases synapse AMPA subunits and ameliorates spatial memory deficits in a mouse model of Alzheimer's disease. *J Neurochem*. 2016; 136:620–36.
<https://doi.org/10.1111/jnc.13432>
PMID:26577931
53. Chen J, Chua KW, Chua CC, Yu H, Pei A, Chua BH, Hamdy RC, Xu X, Liu CF. Antioxidant activity of 7,8-dihydroxyflavone provides neuroprotection against glutamate-induced toxicity. *Neurosci Lett*. 2011; 499:181–5.
<https://doi.org/10.1016/j.neulet.2011.05.054>
PMID:21651962
54. Han X, Zhu S, Wang B, Chen L, Li R, Yao W, Qu Z. Antioxidant action of 7,8-dihydroxyflavone protects PC12 cells against 6-hydroxydopamine-induced cytotoxicity. *Neurochem Int*. 2014; 64:18–23.
<https://doi.org/10.1016/j.neuint.2013.10.018>
PMID:24220540
55. Li XH, Dai CF, Chen L, Zhou WT, Han HL, Dong ZF. 7,8-dihydroxyflavone Ameliorates Motor Deficits Via Suppressing α -synuclein Expression and Oxidative Stress in the MPTP-induced Mouse Model of Parkinson's Disease. *CNS Neurosci Ther*. 2016; 22:617–24.
<https://doi.org/10.1111/cns.12555>
PMID:27079181
56. Liu X, Obianyo O, Chan CB, Huang J, Xue S, Yang JJ, Zeng F, Goodman M, Ye K. Biochemical and biophysical investigation of the brain-derived neurotrophic factor mimetic 7,8-dihydroxyflavone in the binding and activation of the TrkB receptor. *J Biol Chem*. 2014; 289:27571–84.
<https://doi.org/10.1074/jbc.M114.562561>
PMID:25143381
57. Liu C, Chan CB, Ye K. 7,8-dihydroxyflavone, a small molecular TrkB agonist, is useful for treating various BDNF-implicated human disorders. *Transl Neurodegener*. 2016; 5:2.
<https://doi.org/10.1186/s40035-015-0048-7>
PMID:26740873
58. Massa SM, Yang T, Xie Y, Shi J, Bilgen M, Joyce JN, Nehama D, Rajadas J, Longo FM. Small molecule BDNF mimetics activate TrkB signaling and prevent neuronal degeneration in rodents. *J Clin Invest*. 2010; 120:1774–85.
<https://doi.org/10.1172/JCI41356>
PMID:20407211
59. Biancalana M, Koide S. Molecular mechanism of Thioflavin-T binding to amyloid fibrils. *Biochim Biophys Acta*. 2010; 1804:1405–12.
<https://doi.org/10.1016/j.bbapap.2010.04.001>
PMID:20399286
60. Chiu YJ, Lin TH, Chen CM, Lin CH, Teng YS, Lin CY, Sun YC, Hsieh-Li HM, Su MT, Lee-Chen GJ, Lin W, Chang KH. Novel Synthetic Coumarin-Chalcone Derivative (E)-3-(3-(4-(Dimethylamino)Phenyl)Acryloyl)-4-Hydroxy-2H-Chromen-2-One Activates CREB-Mediated Neuroprotection in A β and Tau Cell Models of Alzheimer's Disease. *Oxid Med Cell Longev*. 2021; 2021:3058861.
<https://doi.org/10.1155/2021/3058861>
PMID:34812274
61. Li N, Liu JH, Zhang J, Yu BY. Comparative evaluation of cytotoxicity and antioxidative activity of 20 flavonoids. *J Agric Food Chem*. 2008; 56:3876–83.
<https://doi.org/10.1021/jf073520n>
PMID:18433100
62. Verdonk ML, Cole JC, Hartshorn MJ, Murray CW, Taylor RD. Improved protein-ligand docking using GOLD. *Proteins*. 2003; 52:609–23.
<https://doi.org/10.1002/prot.10465>
PMID:12910460
63. Nissink JW, Murray C, Hartshorn M, Verdonk ML, Cole JC, Taylor R. A new test set for validating predictions of protein-ligand interaction. *Proteins*. 2002; 49:457–71.
<https://doi.org/10.1002/prot.10232>
PMID:12402356
64. Lin CH, Hsieh YS, Wu YR, Hsu CJ, Chen HC, Huang WH, Chang KH, Hsieh-Li HM, Su MT, Sun YC, Lee GC, Lee-Chen GJ. Identifying GSK-3 β kinase inhibitors of Alzheimer's disease: Virtual screening, enzyme, and cell assays. *Eur J Pharm Sci*. 2016; 89:11–9.
<https://doi.org/10.1016/j.ejps.2016.04.012>
PMID:27094783
65. Banfield MJ, Naylor RL, Robertson AG, Allen SJ, Dawbarn D, Brady RL. Specificity in Trk receptor:neurotrophin interactions: the crystal structure of TrkB-d5 in complex with neurotrophin-4/5. *Structure*. 2001; 9:1191–9.
[https://doi.org/10.1016/s0969-2126\(01\)00681-5](https://doi.org/10.1016/s0969-2126(01)00681-5)
PMID:11738045
66. Urfer R, Tsoulfas P, O'Connell L, Shelton DL, Parada LF, Presta LG. An immunoglobulin-like domain determines the specificity of neurotrophin receptors. *EMBO J*. 1995; 14:2795–805.
<https://doi.org/10.1002/j.1460-2075.1995.tb07279.x>
PMID:7796806
67. Chitranshi N, Gupta V, Kumar S, Graham SL. Exploring

- the Molecular Interactions of 7,8-Dihydroxyflavone and Its Derivatives with TrkB and VEGFR2 Proteins. *Int J Mol Sci.* 2015; 16:21087–108.
<https://doi.org/10.3390/ijms160921087>
PMID:[26404256](https://pubmed.ncbi.nlm.nih.gov/26404256/)
68. Pålman S, Ruusala AI, Abrahamsson L, Mattsson ME, Esscher T. Retinoic acid-induced differentiation of cultured human neuroblastoma cells: a comparison with phorbol ester-induced differentiation. *Cell Differ.* 1984; 14:135–44.
[https://doi.org/10.1016/0045-6039\(84\)90038-1](https://doi.org/10.1016/0045-6039(84)90038-1)
PMID:[6467378](https://pubmed.ncbi.nlm.nih.gov/6467378/)
69. Huang CC, Chang KH, Chiu YJ, Chen YR, Lung TH, Hsieh-Li HM, Su MT, Sun YC, Chen CM, Lin W, Lee-Chen GJ. Multi-Target Effects of Novel Synthetic Coumarin Derivatives Protecting A β -GFP SH-SY5Y Cells against A β Toxicity. *Cells.* 2021; 10:3095.
<https://doi.org/10.3390/cells10113095>
PMID:[34831318](https://pubmed.ncbi.nlm.nih.gov/34831318/)
70. Ottaviani G, Martel S, Escarala C, Nicolle E, Carrupt PA. The PAMPA technique as a HTS tool for partition coefficients determination in different solvent/water systems. *Eur J Pharm Sci.* 2008; 35:68–75.
<https://doi.org/10.1016/j.ejps.2008.06.006>
PMID:[18620049](https://pubmed.ncbi.nlm.nih.gov/18620049/)